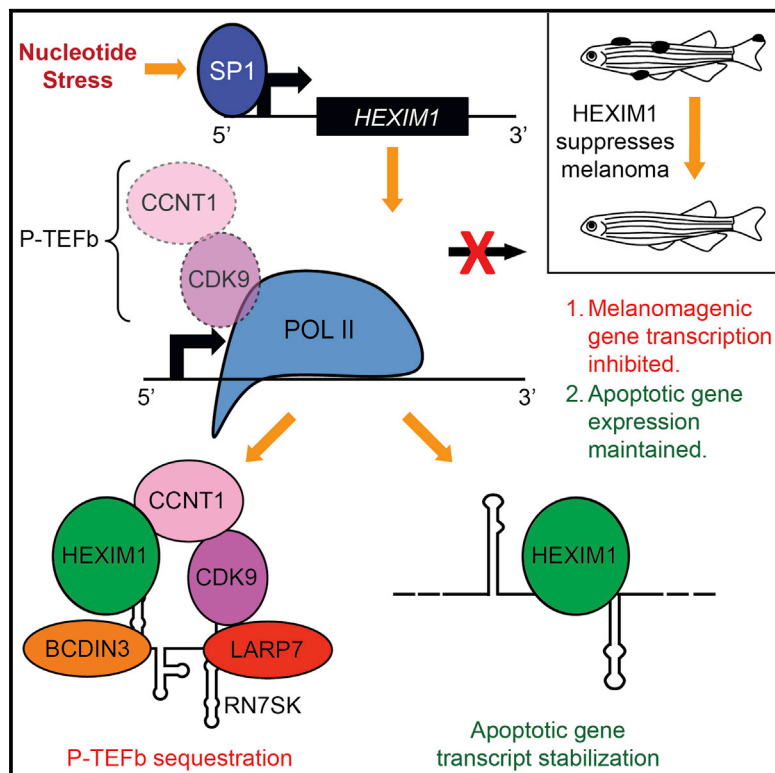


Molecular Cell

Stress from Nucleotide Depletion Activates the Transcriptional Regulator HEXIM1 to Suppress Melanoma

Graphical Abstract



Authors

Justin L. Tan, Rachel D. Fogley, Ryan A. Flynn, ..., Howard Y. Chang, Richard A. Young, Leonard I. Zon

Correspondence

zon@enders.tch.harvard.edu

In Brief

Tan et al. demonstrate that the gene *HEXIM1* is a tumor suppressor in melanoma that responds to nucleotide stress by inhibiting transcription elongation of tumorigenic genes and stabilizing mRNA transcripts of other tumor suppressor genes. These results suggest an important paradigm for targeting melanoma through metabolic stress-induced transcription regulation.

Highlights

- *HEXIM1* is a tumor suppressor in melanoma that responds to nucleotide stress
- In nucleotide stress, *HEXIM1* sequesters P-TEFb to inhibit oncogenic transcription
- *HEXIM1* binds and stabilizes anti-tumorigenic transcripts under nucleotide stress

Accession Numbers

GSE68053



Stress from Nucleotide Depletion Activates the Transcriptional Regulator HEXIM1 to Suppress Melanoma

Justin L. Tan,^{1,2} Rachel D. Fogley,^{1,2} Ryan A. Flynn,³ Julien Ablain,^{1,2} Song Yang,^{1,2} Violaine Saint-André,⁴ Zi Peng Fan,⁴ Brian T. Do,³ Alvaro C. Laga,⁵ Koh Fujinaga,⁶ Cristina Santoriello,^{1,2} Celeste B. Greer,⁷ Yoon Jung Kim,⁸ John G. Clohessy,^{9,10} Anne Bothmer,⁹ Nicole Pandell,¹⁰ Serine Avagyan,^{1,2} John E. Brogie,¹¹ Ellen van Rooijen,^{1,2} Elliott J. Hagedorn,^{1,2} Ng Shyh-Chang,¹² Richard M. White,¹³ David H. Price,¹¹ Pier Paolo Pandolfi,⁹ B. Matija Peterlin,⁶ Yi Zhou,^{1,2} Tae Hoon Kim,⁸ John M. Asara,¹⁴ Howard Y. Chang,³ Richard A. Young,⁴ and Leonard I. Zon^{1,2,*}

¹Howard Hughes Medical Institute, Stem Cell Program and Division of Pediatric Hematology/Oncology, Boston Children's Hospital, Dana-Farber Cancer Institute, Harvard Medical School, Boston, MA 02115, USA

²Department of Stem Cell and Regenerative Biology, Harvard Stem Cell Institute, Cambridge, MA 02138, USA

³Center for Personal Dynamic Regulomes, Stanford University School of Medicine, Stanford, CA 94305, USA

⁴Whitehead Institute for Biomedical Research and Department of Biology, Massachusetts Institute of Technology, Cambridge, MA 02142, USA

⁵Department of Pathology, Brigham & Women's Hospital, Boston, MA 02215, USA

⁶Departments of Medicine, Microbiology, and Immunology, University of California, San Francisco, San Francisco, CA 94143, USA

⁷Department of Pharmacology, School of Medicine, Yale University, New Haven, CT 06520, USA

⁸Department of Biological Sciences, The University of Texas at Dallas, Richardson, TX 75080, USA

⁹Cancer Research Institute, Beth Israel Deaconess Cancer Center, and Department of Medicine and Pathology, Beth Israel Deaconess Medical Center, Harvard Medical School, Boston, MA 02115, USA

¹⁰Preclinical Murine Pharmacogenetics Facility, Beth Israel Deaconess Medical Center, Harvard Medical School, Boston, MA 02115, USA

¹¹Department of Biochemistry, University of Iowa, Iowa City, IA 52242, USA

¹²Genome Institute of Singapore, 60 Biopolis Street, Singapore 138672, Singapore

¹³Memorial Sloan Kettering Cancer Center and Weill Cornell Medical College, New York, NY 10065, USA

¹⁴Division of Signal Transduction, Department of Medicine, Beth Israel Deaconess Medical Center, Harvard Medical School, Boston, MA 02215, USA

*Correspondence: zon@enders.tch.harvard.edu

<http://dx.doi.org/10.1016/j.molcel.2016.03.013>

SUMMARY

Studying cancer metabolism gives insight into tumorigenic survival mechanisms and susceptibilities. In melanoma, we identify HEXIM1, a transcription elongation regulator, as a melanoma tumor suppressor that responds to nucleotide stress. *HEXIM1* expression is low in melanoma. Its overexpression in a zebrafish melanoma model suppresses cancer formation, while its inactivation accelerates tumor onset in vivo. Knockdown of *HEXIM1* rescues zebrafish neural crest defects and human melanoma proliferation defects that arise from nucleotide depletion. Under nucleotide stress, HEXIM1 is induced to form an inhibitory complex with P-TEFb, the kinase that initiates transcription elongation, to inhibit elongation at tumorigenic genes. The resulting alteration in gene expression also causes anti-tumorigenic RNAs to bind to and be stabilized by HEXIM1. HEXIM1 plays an important role in inhibiting cancer cell-specific gene transcription while also facilitating anti-cancer gene expression. Our study reveals an important role for HEXIM1 in coupling nucleotide metabolism with transcriptional regulation in melanoma.

INTRODUCTION

The ability of cancer cells to alter metabolism to enhance survival and adapt to the microenvironment has been studied to understand tumorigenic mechanisms that can be therapeutically targeted. Nucleotide metabolism is dysregulated in cancer. Imbalances in nucleotide pools alter mutation rates (Meuth, 1989; Weinberg et al., 1981). Dysregulation of the nucleotide biosynthesis precursors glycine and glutamine in tumorigenesis invoke changes in nucleotide metabolism (Liu et al., 2012; Zhang et al., 2012). Genetic mutations with altered nucleotide metabolism cause chromosomal instability (Chabosseau et al., 2011; Chang et al., 2013). Our previous work found that inhibition of de novo pyrimidine biosynthesis enzyme dihydro-ototate dehydrogenase (DHODH), by drug leflunomide (lef), ablates zebrafish neural crest and suppresses melanoma through an unclear transcription elongation mechanism (White et al., 2011).

Control of the elongation phase of RNA polymerase II (Pol II) transcription regulates gene expression during differentiation (Guo and Price, 2013). After initiation, Pol II becomes paused at the promoter by negative transcription elongation factors such as DSIF and NELF (Muse et al., 2007; Rahl et al., 2010). Release of these promoter-proximal paused polymerases into productive elongation requires positive transcription elongation factor b (P-TEFb) (Marshall et al., 1996). P-TEFb, comprising cyclin-dependent kinase 9 (CDK9) and either cyclin T1 or T2

(CCNT1/2), phosphorylates Pol II (Marshall et al., 1996), DSIF (Yamada et al., 2006), and NELF (Fujinaga et al., 2004). This releases NELF from the elongation complex and converts DSIF into a positive factor (Fujinaga et al., 2004; Yamada et al., 2006), resulting in productive elongation (Rahl et al., 2010).

The 7SK small nuclear ribonucleoprotein particle (snRNP) critically regulates transcription elongation by sequestering and inactivating P-TEFb (Peterlin et al., 2012). Negative regulation of P-TEFb by HEXIM1 in the 7SK snRNP is essential for regulating gene expression. HEXIM1 binds to 7SK RNA and sequesters P-TEFb in an inactive state (Yik et al., 2003). 7SK snRNP components MEPCE (bcdin3) (Jeronimo et al., 2007) and LARP7 (He et al., 2008) maintain 7SK stability. Regulated release of P-TEFb from the 7SK snRNP is important for rapid gene induction for metazoan development. 7SK snRNP disruption leads to developmental abnormalities in zebrafish (Barboric et al., 2009) and humans (Alazami et al., 2012).

To determine how nucleotide metabolism affects transcription in tumors, we examined the relevance of negative regulators of transcription elongation in cancer and found that *HEXIM1* features significantly in melanoma. Our analysis revealed that *HEXIM1* mRNA and protein levels are low in melanoma. In vivo studies demonstrate that *HEXIM1* functions as a melanoma suppressor: its overexpression suppresses tumor onset, while its inactivation accelerates tumorigenesis. Pyrimidine nucleotide depletion induces SP1-mediated *HEXIM1* upregulation to suppress melanocyte and neural crest formation in vivo. Under nucleotide stress, *HEXIM1* forms an inhibitory complex with P-TEFb, inhibiting productive elongation at neural crest-associated and tumorigenic genes. The alteration in gene expression causes anti-tumorigenic transcripts to bind to and become stabilized by *HEXIM1*. *HEXIM1* induction by nucleotide stress facilitates a gene expression switch, inhibiting tumorigenic gene transcription while favoring anti-tumorigenic gene transcription. The ability of *HEXIM1* to couple nucleotide stress with an anti-melanoma transcriptional response is an important mechanism in tumor metabolism.

RESULTS

HEXIM1 Expression Is Low in Melanoma

We evaluated the role of candidate transcription elongation regulators in Oncomine (Rhodes et al., 2004) and only *HEXIM1* expression was significantly altered in melanoma (data not shown). We analyzed two human melanoma microarray datasets for *HEXIM1* expression (Lin et al., 2008; Talantov et al., 2005). Talantov et al. (2005) studied gene expression from primary melanoma and benign skin nevi, while Lin et al. (2008) examined gene expression in melanoma short-term cultures and cell lines. *HEXIM1* is downregulated by at least 2-fold in 78% of nevi compared to normal skin controls (Figures 1A and S1A). Comparing melanoma and skin, *HEXIM1* was downregulated in 100% of melanoma cases by at least 2-fold (Figures 1A and S1A). In short-term cultures and cell lines versus normal melanocyte lines, 44% of melanoma cases had *HEXIM1* downregulated by at least 2-fold (Figures 1B and S1A). Other 7SK snRNP members were not significantly downregulated (Figure S1B). *HEXIM1* is likely downregulated in melanoma.

To assess *HEXIM1* protein levels, we performed immunohistochemistry on human melanoma tissue microarrays. We scored them by the H-score method on a scale of 0 to 300 (McClelland et al., 1990); 66% of nevi and 72% of human melanoma samples showed low H-scores of <100, corresponding to low *HEXIM1* protein levels (Figures 1C and S1C). Also, 6% of nevi and 13% of melanoma showed high *HEXIM1* levels with H-scores of >200 (Figures S1C and S1D), and 100% of normal epidermal samples scored high for *HEXIM1* expression, with 94% of samples possessing H-scores of >200 (Figures S1C and S1D). As melanoma is derived from melanocytes, we examined normal epidermal sections co-stained for *HEXIM1* and MART1, a melanocyte-specific cell surface antigen (Kawakami et al., 1994). Melanocytes co-expressed high levels of both MART1 and *HEXIM1*, meaning that *HEXIM1* protein levels are high in normal melanocytes compared to nevi and melanoma (Figure S1E). These results suggest that *HEXIM1* protein is downregulated in melanoma.

There are no significant mutations in the *HEXIM1* gene across tumor databases (data not shown), suggesting that, in melanoma, epigenetic silencing might cause *HEXIM1* downregulation. We examined DNA methylation of the *HEXIM1* locus using MethHC (Huang et al., 2015) to analyze melanoma methylation data from The Cancer Genome Atlas (TCGA). The *HEXIM1* promoter is hypermethylated in tumor samples, suggesting that hypermethylation downregulates *HEXIM1* (Figure 1D). To functionally test if the *HEXIM1* promoter is methylated in melanoma, we treated the human A375 melanoma cell line with 5-azacytidine, a DNA methyltransferase (DNMT) inhibitor that removes methylation on DNA (Creusot et al., 1982). We observed a dose-dependent upregulation of *HEXIM1* transcripts (Figure 1E) and reduced cell viability (Figure 1F) with DNMT inhibition. Together, the expression patterns and epigenetic silencing by DNA methylation suggest that *HEXIM1* is a tumor suppressor that is downregulated in melanoma.

HEXIM1 Overexpression Suppresses Melanoma Onset while Its Inactivation Accelerates Melanoma In Vivo

To investigate the in vivo action of *HEXIM1* on melanoma, we overexpressed human *HEXIM1* and zebrafish *hexim1* in the MiniCoopR zebrafish assay system (Ceol et al., 2011). Compared to the *EGFP* background control and the *SETDB1* positive control, which accelerates tumor onset, both human *HEXIM1* and fish *hexim1* suppressed melanoma onset (Figures 2A and 2B). Of the *HEXIM1/hexim1* fish, 80% remained tumor free at the 25-week endpoint, while 30% of *EGFP* and 10% of *SETDB1* fish were tumor free.

We investigated if *HEXIM1* suppression of tumorigenesis is dependent on its P-TEFb sequestration function. *HEXIM1*/P-TEFb interaction is modulated by mutating *HEXIM1* amino acid residues at S268, T270, T276, and S278, located at the P-TEFb-binding domain (Contreras et al., 2007). Mutating these sites to aspartic acid generates *HEXIM1-4D*, which ablates P-TEFb binding. Mutating these sites to alanine generates *HEXIM1-4A*, which efficiently sequesters P-TEFb. Overexpressing *HEXIM1-4A* suppresses tumors to a similar extent as *HEXIM1* and *hexim1* (Figure 2C). Overexpressing *HEXIM1-4D* did not suppress tumors and tumorigenesis continued at a

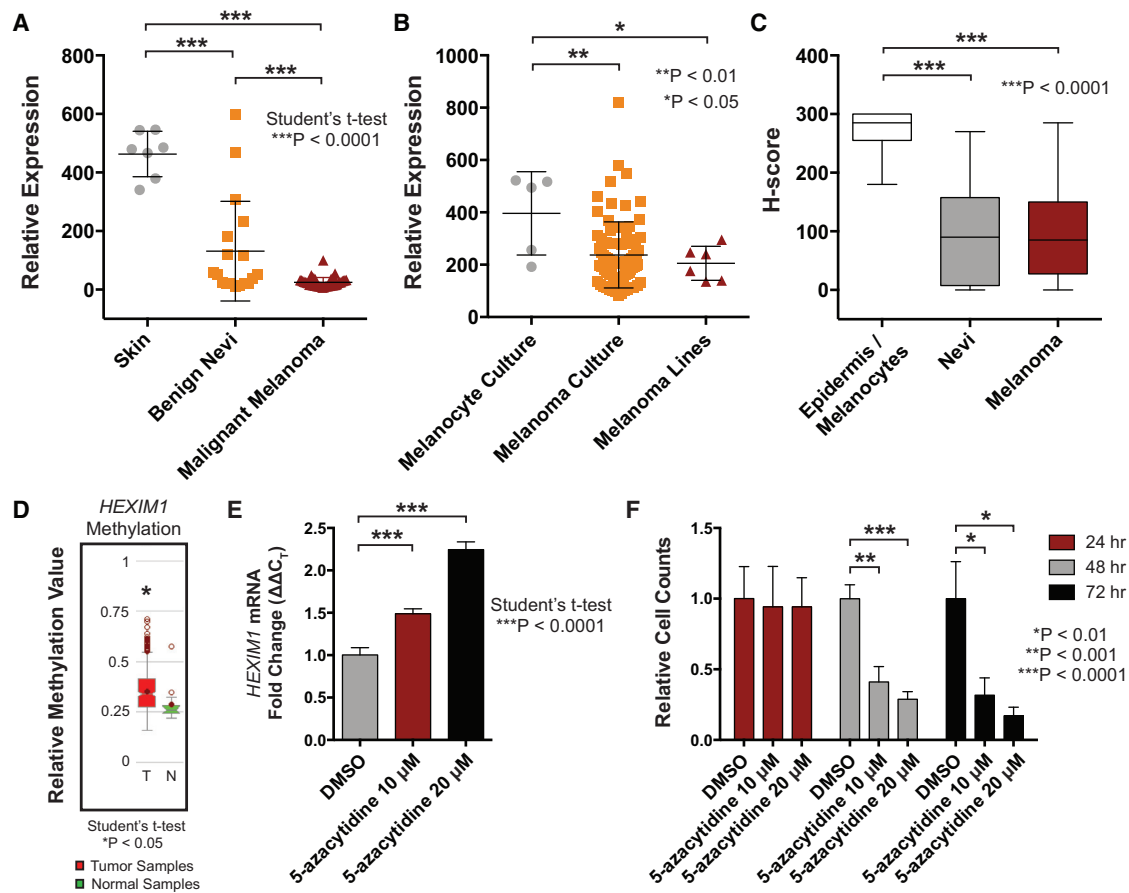


Figure 1. *HEXIM1* Is Downregulated in Melanoma

(A) Gene expression plot of *HEXIM1* microarray data from Talantov et al. (2005) comparing nevi/tumor samples versus normal skin controls. The data are represented as mean ± SD.

(B) Gene expression plot of *HEXIM1* microarray data from Lin et al. (2008) compares primary melanoma cultures and melanoma cell lines to melanocyte culture controls (mean ± SD).

(C) Bar graph shows H-scores for normal epidermis, nevi, and melanoma samples (mean ± SD).

(D) *HEXIM1* locus methylation plot for TCGA skin cutaneous melanoma samples, analyzed by MethHC, is shown (mean ± SD).

(E) Real-time RT-PCR for *HEXIM1* expression in A375 cells treated with 5-azacytidine for 24 hr normalized to *GAPDH* is shown (mean of three replicates ± SD).

(F) Cell number of A375 cells treated with 5-azacytidine for 24–72 hr relative to DMSO controls is shown (mean of three replicates ± SD).

See also Figure S1.

similar rate to *EGFP* (Figure 2C). We validated MiniCoopR transgenic construct expression by sequencing and western blots (Figures S2A–S2C).

We investigated the effects of *HEXIM1* overexpression in melanocytes during development. We outcrossed *HEXIM1*, *HEXIM1-4A*, and *-4D* MiniCoopR transgenic fish to the *Tg(mitfa:BRAF^{V600E});p53^{-/-};mitfa^{-/-}* parental strain and examined melanocytes at 2 days post-fertilization (dpf), using a Tu wild-type strain incross as control (Figure S2D). The outcrosses for the *HEXIM1* and *HEXIM1-4D* strains produced offspring with an embryonic decrease in melanocytes, similar to DHODH inhibition effects (White et al., 2011). This melanocyte reduction did not occur for the *EGFP* or *HEXIM1-4D* strains. These studies show that the capacity of *HEXIM1* to sequester P-TEFb is required for its function in tumor suppression and development.

To analyze the effect of *HEXIM1* inactivation in vivo, we employed a CRISPR/Cas9 knockout of *hexim1* in our zebrafish melanoma model. Under control of the MiniCoopR vector, we expressed *hexim1* and *p53* control guide RNAs (gRNAs) and Cas9 in a melanocyte-specific fashion (Ablain et al., 2015) to examine tumor onset. Since the *Tg(mitfa:BRAF^{V600E});p53^{-/-};mitfa^{-/-}* fish have non-functional *p53*, the *p53* CRISPR controls for random targeting events. Mutation of the *hexim1* gene was confirmed by a T7E1 enzymatic genotyping assay, and western blot showed lower *hexim1* protein levels (Figures S2E and S2F). Reduced *hexim1* expression due to heterozygous inactivation resulted in accelerated tumor onset compared to the *p53* control (Figure 2D), consistent with *HEXIM1* functioning as a tumor suppressor.

We examined the tumor-suppressive ability of *HEXIM1* in a mouse xenograft model with a Tet-On *HEXIM1*-inducible A375

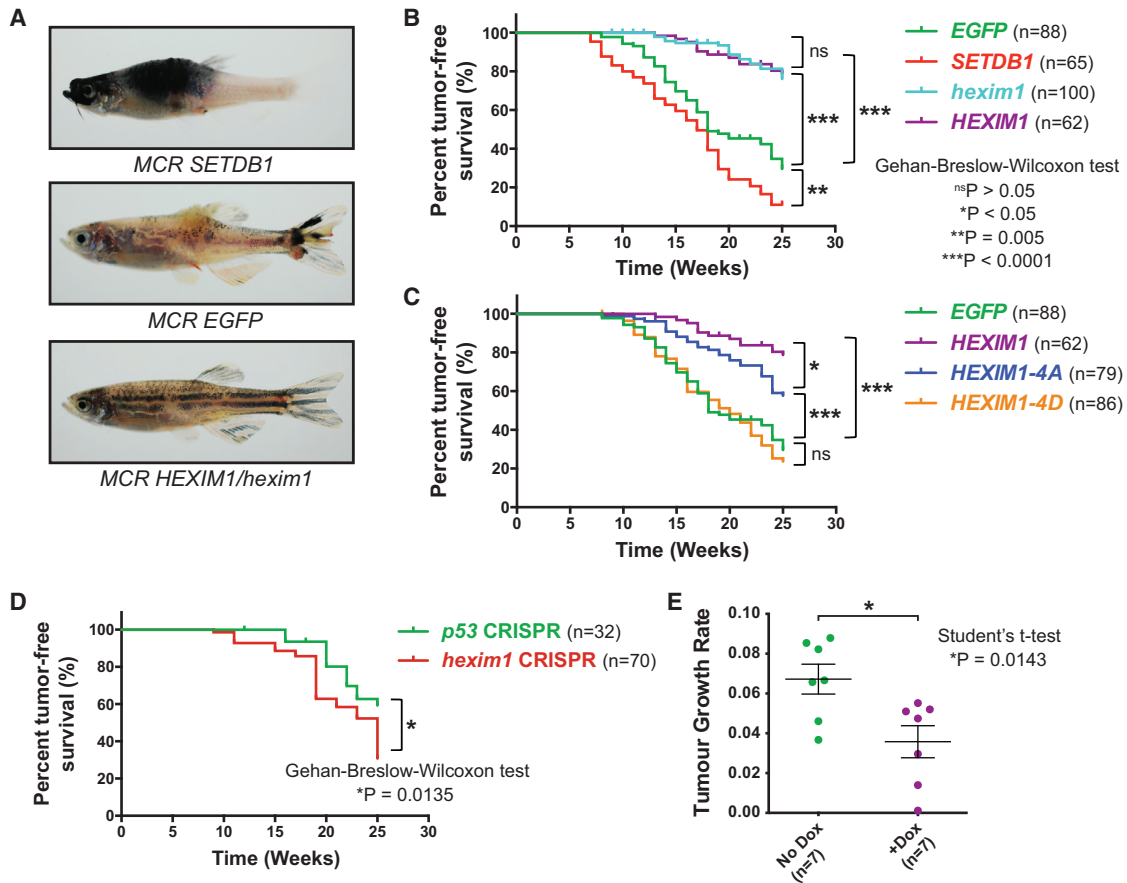


Figure 2. *HEXIM1* Activity Suppresses Melanoma In Vivo

(A) 19-week-old *Tg(mitfa:BRAF^{V600E});p53^{-/-};mitfa^{-/-}* zebrafish are shown with rescued melanocytes expressing tumor accelerator *SETDB1*, background control *EGFP*, or *HEXIM1/hexim1* in the MiniCoopR system.

(B) Tumor-free survival curves for *EGFP*, *SETDB1*, and *HEXIM1/hexim1* MiniCoopR zebrafish over 25 weeks. Percentages of the total number of zebrafish that were tumor free each week are plotted.

(C) Tumor-free survival curves for MiniCoopR overexpression of human *HEXIM1-4A*, and *HEXIM1-4D* are shown.

(D) Tumor-free survival curves for MiniCoopR expression of *p53* and *hexim1* CRISPRs are shown.

(E) Tumor growth rates of individual mouse xenografts with a Tet-On *HEXIM1*-inducible A375 cell line (A375-*HEXIM1*) over 14 days. Mice were fed either a standard diet or doxycycline diet (mean of seven replicates \pm SD).

See also Figure S2.

melanoma cell line (A375-*HEXIM1*). *HEXIM1* induction with a doxycycline diet significantly reduced tumor growth rates compared to uninduced mice (Figures 2E and S2G), complementing our fish data that *HEXIM1* is a melanoma suppressor.

Knockdown of *HEXIM1* Rescues Neural Crest and Melanoma Phenotypes Associated with Nucleotide Stress

DHODH inhibition by *lef* ablates *crestin* (neural crest marker) and *mitfa* (master regulator of melanocyte fate) gene expression in developing zebrafish embryos (White et al., 2011). *Hexim1* morpholino knockdown partially rescued *crestin* and *mitfa* expression in *lef*-treated zebrafish embryos (Figure 3A). Melanocytes were partially rescued (Figures 3B and 3C). Overexpressing human *HEXIM1*, via mRNA injection, with zebrafish *hexim1* knockdown ablated the rescue. We validated *hexim1* protein

knockdown via western blot (Figure S3A). *Hexim1* is ubiquitously expressed in early zebrafish development (Figures S3B–S3D). Knockdown of the 7SK snRNP members *larp7* and *mepce* recapitulated the rescue of melanocytic gene expression and melanocytes seen in *hexim1* knockdown (Figures S3E and S3F). We observed melanocyte reduction in our *HEXIM1*-overexpressing zebrafish embryos (Figure S2D) similar to the *lef* embryonic phenotype. However, this was only a partial phenocopy of *lef* since *crestin* expression was unchanged (data not shown), possibly because *HEXIM1* is specifically overexpressed in melanocytes under the *mitfa* promoter and the early neural crest cells affected by *lef* are still present in the transgenic embryos. *Hexim1* plays a role in neural crest in vivo effects caused by nucleotide stress.

DHODH inhibition causes growth arrest in the human A375 melanoma cell line (White et al., 2011). We performed pooled

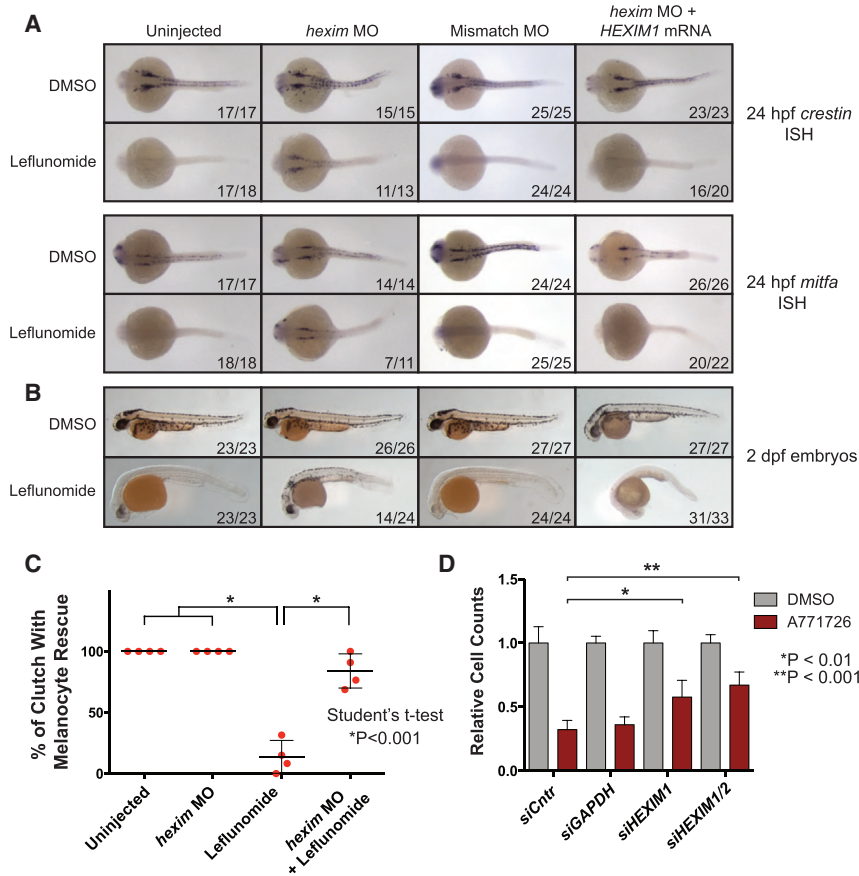


Figure 3. Knockdown of *HEXIM1* Rescues Nucleotide Stress-Associated Neural Crest Ablation and Melanoma Suppression Phenotypes

(A) Zebrafish embryos were injected with 8 ng *hexim1* or control morpholino (MO) or a combination of *hexim1* MO and 300 pg human *HEXIM1* mRNA. Embryos were treated with DMSO or 6.5 μ M lef at 50% epiboly and in situ hybridization was performed at 24 hr post-fertilization (hpf) for *crestin* or *mitfa* expression. Dorsal views of embryos are shown. Numbers indicate the number of embryos with the shown phenotype versus the total number of embryos in the clutch.

(B) Embryos treated as in (A) were scored for melanocytes at 2 dpf.

(C) Four clutches of embryos were analyzed for rescue of melanocytes under the conditions of uninjected, *hexim1* MO injected, lef treatment, or *hexim1* MO injected with lef treatment. Percentages of the number of embryos rescued in each clutch are plotted (mean \pm SD).

(D) Cell number of A375 cells treated with 25 μ M A771726 in combination with siRNA pools for *GAPDH*, *HEXIM1*, and *HEXIM2* relative to DMSO controls is shown (mean of three replicates \pm SD). See also Figure S3.

small interfering RNA (siRNA) knockdown of *HEXIM1* on A375 cells treated with A771726, and we showed a partial rescue of the growth arrest phenotype (Figure 3D). A combined *HEXIM1* and *HEXIM2* knockdown marginally improved rescue, while applying a non-targeting siRNA pool or *GAPDH* knockdown did not rescue (Figure 3D). Knockdowns were validated by RT-PCR (Figure S3G). These results suggest that *HEXIM1* plays an important role in the transcriptional response to nucleotide stress in the neural crest lineage and melanoma.

HEXIM1 Is Upregulated in Response to Nucleotide Stress in Melanoma

Metabolite profiling of A375 cells with metabolized lef, A771726, revealed that pyrimidine biosynthesis- and RNA transcription-associated metabolites were primarily dysregulated (Figure S4A; Table S1). Metabolites upstream of DHODH were upregulated while metabolites downstream of DHODH were downregulated (Figures S4B and S4C). Changes were limited to pyrimidine intermediates before 48 hr, after which secondary effects, such as purine metabolite changes, were observed (Figures S4A and S4C; Table S1). This highlights the specificity of DHODH inhibitors to pyrimidine biosynthesis.

To examine the effect of pyrimidine stress on *HEXIM1* expression, zebrafish embryos and human A375 cells were treated with lef and A771726, respectively. *HEXIM1* was upregulated with drug treatment in both systems in a dose-dependent manner

control hexamethylene bisacetamide (HMBA) that upregulates *HEXIM1* (Figure 4E). *HEXIM1* was upregulated after 48 hr of drug treatment (Figure 4F), when pyrimidine nucleotides were significantly depleted (Figure S4C) and when growth arrest became significant (Figure 4G). Increased *HEXIM1* expression induced by nucleotide stress could be rescued by adding pyrimidine nucleotides to drug-treated cells (Figure 4H). Adding nucleotides alone did not alter *HEXIM1* expression (Figure 4H), suggesting that the role of *HEXIM1* in transcriptional regulation is prominent in times of starvation and not nucleotide excess. Nucleotide starvation activates *HEXIM1* with a corresponding decrease in cell proliferation.

HEXIM1 Is Upregulated by SP1 under Nucleotide Stress

We asked which transcription factor is responsible for *HEXIM1* nucleotide stress upregulation by examining the Encyclopedia of DNA Elements (ENCODE) transcription factor chromatin immunoprecipitation sequencing (ChIP-seq) database (ENCODE Project Consortium, 2012) and selecting eight candidate transcription factors that significantly bind the *HEXIM1* promoter. We screened these factors by siRNA knockdown to determine which one promotes *HEXIM1* upregulation under nucleotide stress (Figure S5A). Knockdown was validated by RT-PCR (Figure S5B). *SP1* knockdown significantly blocked *HEXIM1* upregulation by A771726 treatment (Figures 5A and S5A). *SP1* is a stress response factor (Ryu et al., 2003), and its knockdown partially rescued lef-induced

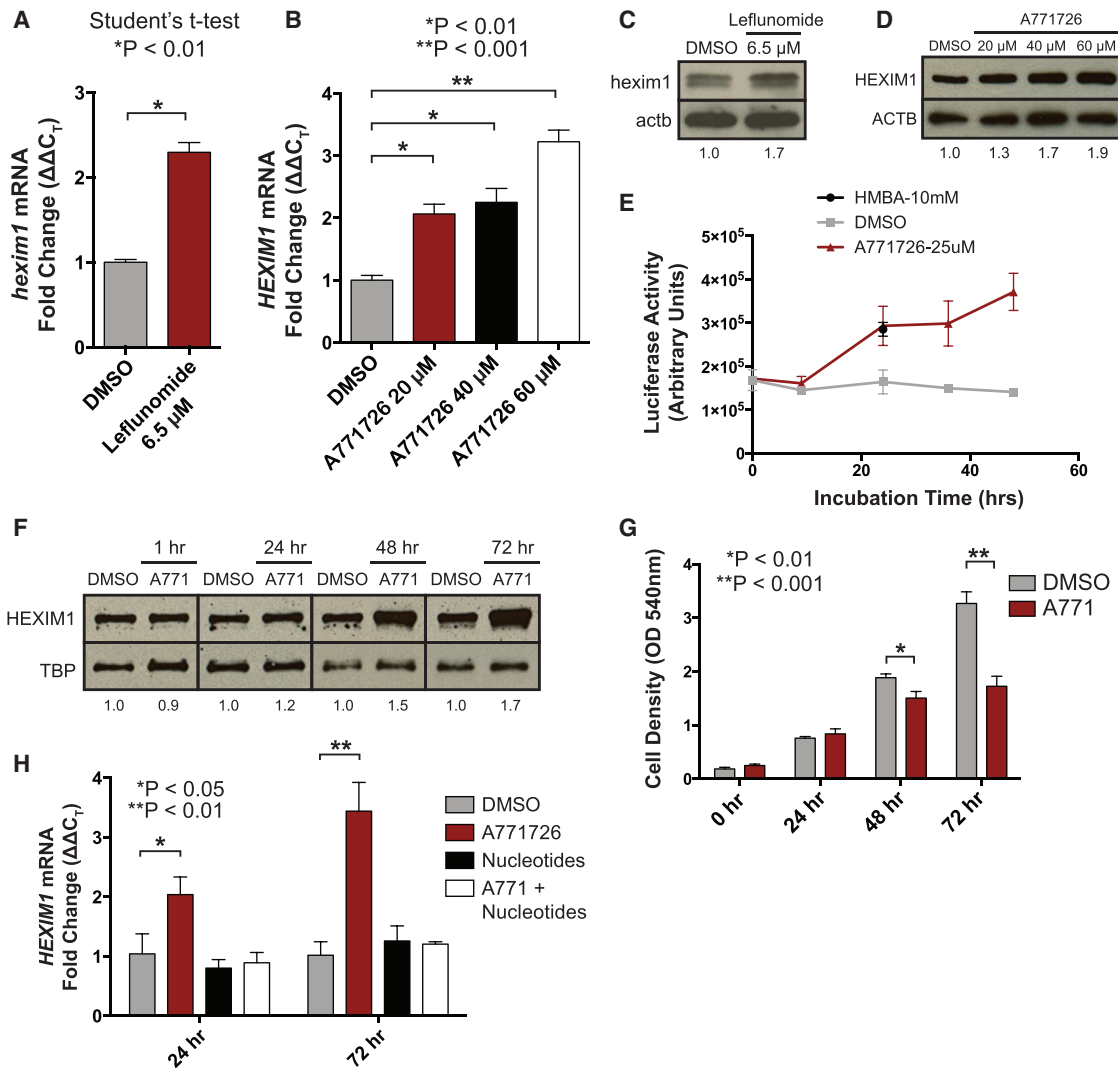


Figure 4. HEXIM1 Is Upregulated by Pyrimidine Nucleotide Stress

(A) Real-time RT-PCR for *hexim1* expression in 24-hpf zebrafish embryos treated with lef normalized to *gapdh* is shown (mean of three replicates \pm SD).
 (B) Real-time RT-PCR for *HEXIM1* expression in A375 cells treated with A771726 for 72 hr normalized to *GAPDH* is shown (mean of three replicates \pm SD).
 (C) Western blot for *hexim1* in 24-hpf zebrafish embryos treated with lef from 50% epiboly to 24 hpf. Numbers represent quantified pixel density of *hexim1* bands relative to DMSO control.
 (D) Western blot for *HEXIM1* in A375 cells treated with A771726 for 72 hr with quantified *HEXIM1* pixel density relative to the DMSO control is shown.
 (E) *HEXIM1*-luciferase reporter assay in A375 cells treated with 10 mM HMBDA, DMSO, or 25 μ M A771726 for 48 hr is shown (mean of two replicates \pm SD).
 (F) Western blot shows *HEXIM1* and TATA-binding protein (TBP) in A375 cells treated with 25 μ M A771726 for 1, 24, 48, and 72 hr with quantified *HEXIM1* pixel density relative to DMSO control.
 (G) Quantification of cell number of A375 cells treated like in (F) is shown (mean of three replicates \pm SD).
 (H) Real-time RT-PCR for *HEXIM1* expression in A375 cells treated with 25 μ M A771726, a cocktail of 10 μ g/ml pyrimidine nucleotides (UMP and CMP), and a combination of both A771726 and nucleotides at 24 and 72 hr normalized to *GAPDH* is shown (mean of three replicates \pm SD).
 See also [Figure S4](#) and [Table S1](#).

growth arrest similar to *HEXIM1* knockdown ([Figure 5B](#)). The *HEXIM1* minimal promoter element used in the luciferase reporter assay in [Figure 4E](#) contains an SP1-binding element ([Liu et al., 2014](#)). ChIP-seq experiments demonstrated that SP1 binding was increased at many loci under nucleotide stress, where some genes were activated while others were repressed by RNA sequencing (RNA-seq, data not shown). The *HEXIM1* promoter is one region where SP1 binding was increased ([Figure 5C](#)),

with an associated increase in *HEXIM1* expression. These data establish a role for SP1 in the upregulation of *HEXIM1* expression under nucleotide stress conditions.

HEXIM1 Induction Sequesters P-TEFb Away from Gene Promoters

We investigated if *HEXIM1* chromatin occupancy is affected by nucleotide stress by performing ChIP-seq for CDK9 and *HEXIM1*

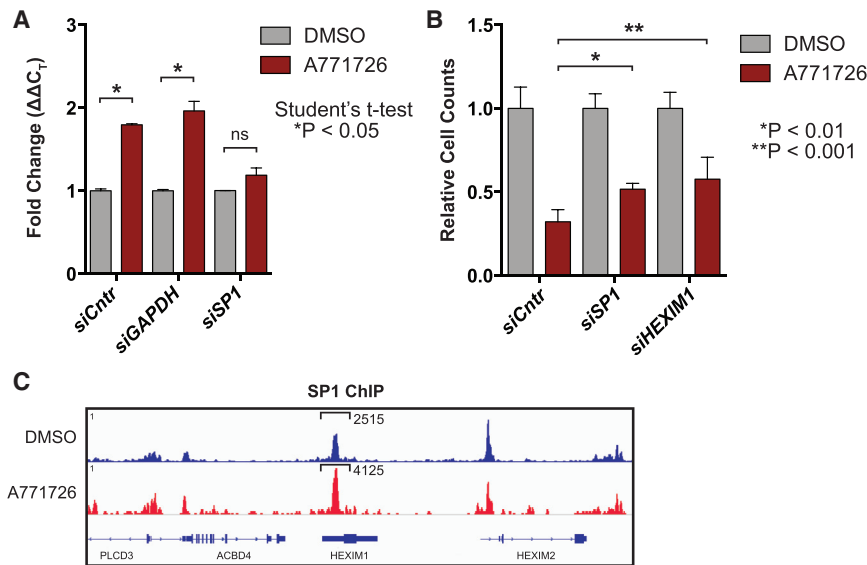


Figure 5. *HEXIM1* Is Upregulated under Nucleotide Stress by SP1

(A) Real-time RT-PCR for *HEXIM1* expression in A375 cells treated with 25 μ M A771726 and pooled siRNAs for non-targeting siRNAs, *GAPDH*, and *SP1* at 48 hr normalized to *ACTB* (mean of three replicates \pm SD). This is a subset of the full screening data in Figure S5A.

(B) Cell number of A375 cells treated with 25 μ M A771726 in combination with a non-targeting siRNA pool, an *SP1* or *HEXIM1* siRNA pool for gene knockdown relative to DMSO controls is shown (mean of three replicates \pm SD).

(C) SP1 ChIP-seq peaks around the *HEXIM1* locus in A375 cells treated with DMSO or A771726. Read density at the *HEXIM1* locus is normalized to all called peaks and quantified.

See also Figure S5.

in A375 cells treated with A771726 for 48 hr. We chose the 48-hr time point since *HEXIM1* protein levels are significantly upregulated (Figure 4F) with no induction of apoptosis (data not shown). It takes 24 hr for lef to downregulate pyrimidines (Figure S4C), after which *HEXIM1* is induced. Pol II ChIP-seq and meta-gene analysis were performed on the same batch of cells to show that drug treatment did not affect immunoprecipitation efficiency (Figure S6A).

Meta-gene analysis demonstrated that CDK9 and *HEXIM1* were localized at gene promoters (Figures 6A and 6B). ChIP-seq region plots for CDK9 and *HEXIM1* binding throughout the genome, based on either CDK9- or *HEXIM1*-binding regions in the DMSO control, showed co-binding of *HEXIM1* with CDK9 at the same regions (Figure 6C). We confirmed this co-binding by performing ChIP-reChIP for *HEXIM1* and CDK9. ChIP-reChIP region and meta-gene plots demonstrated that *HEXIM1* and CDK9 indeed bound at identical chromatin regions (Figures S6B and S6C).

A771726 treatment reduced both CDK9 and *HEXIM1* occupancy at the promoters (Figures 6A and 6B). This reduction could be due to increased *HEXIM1* sequestration of P-TEFb, where coimmunoprecipitation of *HEXIM1* demonstrated that more CDK9 was being incorporated into the 7SK snRNP inhibitory complex with drug (Figure S6D). *HEXIM1* binding to P-TEFb is crucial for its *in vivo* tumor suppression activity and developmental effects (Figures 1H and S2D), which could account for the anti-proliferative effect that A771726 has on melanoma. These data suggest that *HEXIM1* poises P-TEFb at gene promoters for a rapid release to the transcriptional machinery when required. Upon nucleotide stress, *HEXIM1* is induced to sequester P-TEFb to decrease productive elongation.

HEXIM1 Induction Reduces Productive Elongation at Neural Crest and Tumorigenic Genes

To examine the transcriptional effects of *HEXIM1* sequestration of P-TEFb under nucleotide stress, we performed global run-on sequencing (GRO-seq) on A375 cells treated with lef or A771726 at the same time point as our ChIP-seq experiments.

Genes that were considered expressed in the DMSO condition, with a traveling ratio (TR) cutoff of less than 7.5 (White et al., 2011), were used in the GRO-seq analysis for DMSO, lef, and A771726 conditions. TR is a measure of Pol II transcription along a gene in which read density at the promoter is divided by read density along the gene body (Rahl et al., 2010; Zeitlinger et al., 2007). A higher TR corresponds to a decrease in productive elongation. Pol II occupancy at the promoters and gene bodies was plotted for short-listed gene loci in all three conditions (Figure S6E). Overall TRs calculated from Figure S6E showed a significant increase in TR for both lef and A771726 treatment (Figure 6D). Gene meta-analysis showed that Pol II density was lower in the gene body with nucleotide stress (Figure 6E). Pol II promoter density remained largely unchanged (Figure 6E), indicating that productive elongation was reduced with little effect on Pol II promoter-proximal pausing. Example tracks of unaffected housekeeping gene β -actin (*ACTB*) and affected melanoma-associated transcription factor *HMGA2* (Raskin et al., 2013) are shown (Figure S6F). GRO-seq suggests that nucleotide stress reduces productive elongation in melanoma.

To assess *HEXIM1*'s role in the reduction of productive elongation, we examined Serine-2 phosphorylation (Ser2p) of the Pol II C-terminal domain in A375 cells treated with A771726 and with *HEXIM1* pooled knockdown. The transition into productive elongation mediated by P-TEFb leads to increased Ser2p (Adelman and Lis, 2012). In cells with non-targeting siRNA, Ser2p was decreased by 40% with increased *HEXIM1* levels (Figure S6G). We expected this decrease in Ser2p since GRO-seq demonstrated a reduction in productive elongation at actively transcribed genes. Reduced Ser2p was rescued by *HEXIM1* knockdown (Figure S6G). Nucleotide stress also caused a moderate transcription initiation defect, evident from the decrease in initiation marker Serine-5 phosphorylation (Ser5p) that was only partially rescued by *HEXIM1* knockdown (Figure S6G). We induced *HEXIM1* in the A375-*HEXIM1* cell line and observed a 40% decrease in Ser2p similar to A771726

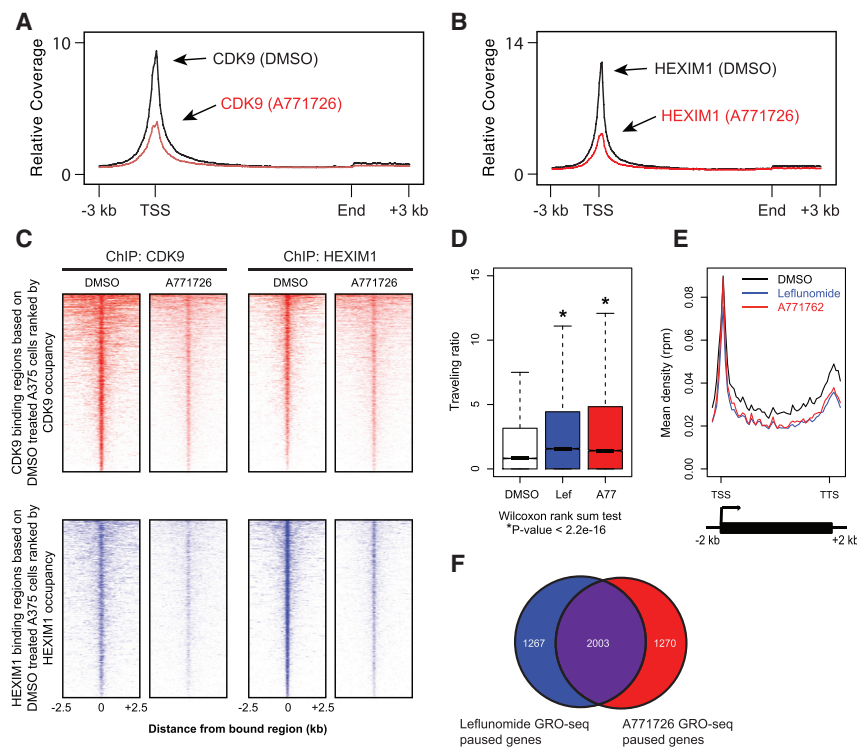


Figure 6. HEXIM1 Reduces Productive Elongation at Tumorigenic Genes by P-TEFb Sequestration under Nucleotide Stress

(A) Metagenesis of all transcribed genes ± 2 kb around transcription units for CDK9-binding regions in DMSO- or A771726-treated (25 μ M for 48 hr) A375 cells is shown.

(B) Metagenesis of all transcribed genes ± 2 kb around transcription units for HEXIM1-binding regions in DMSO- or A771726-treated (25 μ M for 48 hr) A375 cells is shown.

(C) ChIP-seq region plots represent the distribution of regions bound by CDK9 and HEXIM1 in A375 cells, treated with either DMSO or 25 μ M A771726 for 48 hr, ± 2.5 kb relative to all CDK9- or HEXIM1-bound sites in the DMSO-treated A375 cells.

(D) Pol II traveling ratios (TRs) from GRO-seq performed on 48-hr DMSO- (white), 25 μ M lef- (blue), or 25 μ M A771726- (red) treated A375 cells are shown (mean of two replicates \pm SD).

(E) Metagenesis analysis shows Pol II occupancy ± 2 kb around transcription units from GRO-seq described in (D).

(F) Venn diagram of genes in the lef- (blue) or A771726- (red) treated condition that have a Pol II TR fold change of >1.3 .

See also Figure S6 and Table S2.

treatment of endogenous A375 cells (Figure S6H). Ser5p was not significantly affected with *HEXIM1* overexpression (Figure S6H). RNA-seq on this *HEXIM1*-overexpressing line showed a trend of gene expression downregulation (Figure S6I). Gene expression was quantified by the number of fragments per kilobase of transcript per million mapped reads (FPKM), with a cutoff of FPKM > 1 for expressed genes. We curated genes lists for significantly downregulated genes (defined as having an FPKM value of >1 in the uninduced condition, with a corresponding decrease in FPKM upon *HEXIM1* induction by >1.5 -fold) in the *HEXIM1* overexpression RNA-seq (Table S2) and genes with significant reduction in elongation (fold change in TR > 1.3 , drug versus DMSO) in the GRO-seq experiments (Figure 6F). We observed 692 genes that had decreased expression and elongation (Figure S6J). These results suggest that nucleotide stress induces *HEXIM1* to reduce Ser2p and Pol II-mediated transcription elongation.

To examine how nucleotide stress-induced elongation inhibition suppresses melanoma, we performed ingenuity pathway analysis (IPA) on the overlapping 2,003 GRO-seq genes with significant reduction in elongation (Figure 6F; Table S2). Genes involved in gene expression, cell proliferation, and cell death were enriched (Table S2). We also performed IPA on a 137-gene list obtained from overlapping the GRO-seq list with our previously published Pol II ChIP-seq list (Figure S6K; Table S2), which showed enrichment in cell cycle and proliferation pathways (Table S2). A list of 368 neural crest-associated genes was generated based on literature (Table S2) and compared to GRO-seq elongation-inhibited genes in Figure 6F; 33 neural crest-associated genes, including known melanoma oncogenes, had significantly reduced elongation by GRO-seq (Table

S2). Through transcription factor motif analysis, MYC target genes were preferentially elongation inhibited (Figure S6L), as reported in our previous study (White et al., 2011). These data suggest that nucleotide stress induces *HEXIM1* to suppress melanoma by reducing productive elongation at genes associated with melanoma progression.

HEXIM1 Binds Anti-tumorigenic Transcripts under Nucleotide Stress

To survey global *HEXIM1* RNA targets and determine if nucleotide stress causes changes in these RNA interactions, we performed fully automated and standardized individual-nucleotide resolution cross-linking and immunoprecipitation (FAST-iCLIP) (Flynn et al., 2015) on *HEXIM1* with A771726 treatment in A375 cells (Figure S7A). The proportion of 7SK bound to *HEXIM1* did not change significantly with drug (data not shown). We detected significant changes in mRNA transcripts bound to *HEXIM1* (Figure 7A). Transcripts from 2,012 genes were prominently bound by *HEXIM1* at steady state. Upon nucleotide stress induction, 1,063 transcripts were no longer detected while 875 new gene transcripts were bound (Figure 7A). We observed 232 transcripts with increased binding, while 299 transcripts had decreased binding (Figure 7A). Example transcripts of *CDKN1A* and *PTEN* were increasingly bound by *HEXIM1* under nucleotide stress, while there was no change for *CCNT2* transcripts (Figure 7B). *HEXIM1* RNA binding changes dynamically on specific gene transcripts although others remain unaffected.

To discern the biological consequence of altered *HEXIM1* binding of mRNAs, we performed RNA-seq on A375 cells at various A771726 treatment time points as well as a DMSO control 72-hr treatment to compare the changes in gene

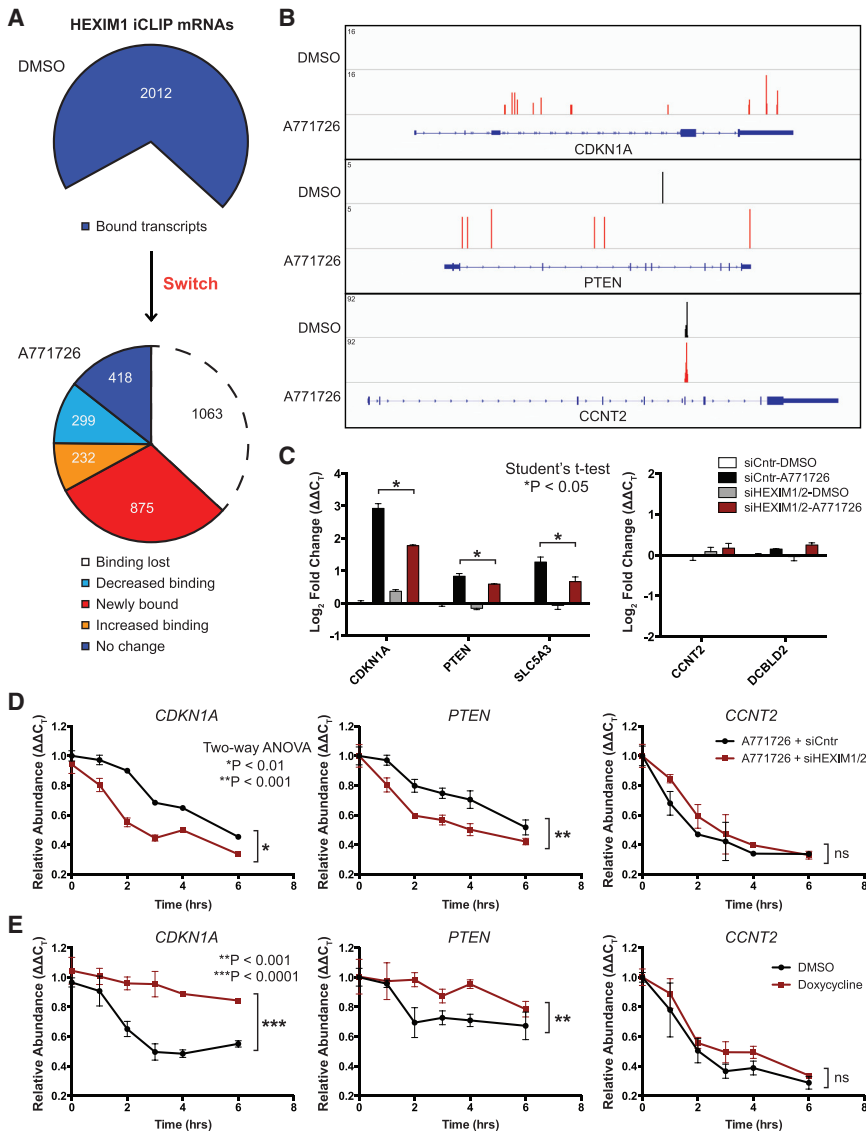


Figure 7. HEXIM1 Binds and Maintains Levels of Anti-tumorigenic Transcripts under Nucleotide Stress

(A) Pie charts summarize the switch in mRNAs bound by HEXIM1 in response to nucleotide depletion.

(B) FAST-iCLIP RT-stops represent regions of HEXIM1 binding mapped to three representative genes.

(C) Real-time RT-PCR on A375 cells treated with 25 μM A771726 and a combination of *HEXIM1* and *HEXIM2* pooled siRNAs to examine expression in three genes upregulated by nucleotide depletion and increasingly bound by HEXIM1 (*CDKN1A*, *PTEN*, and *SLC5A3*), and two genes unchanged by nucleotide depletion and with no change in HEXIM1 binding (*CCNT2* and *DCBLD2*) (mean of three replicates ± SD). Data are normalized to *RPL11*.

(D) RNA stability assay where A375 cells were first treated with either 25 μM A771726 or 25 μM A771726 in combination with siRNA knockdown of *HEXIM1* and *HEXIM2* for 48 hr, followed by 5 μg/ml actinomycin D treatment. RNA was isolated at various time points after actinomycin D treatment and relative mRNA abundance over time is plotted for *CDKN1A*, *PTEN*, and *CCNT2* (mean of three replicates ± SD). Data are normalized to *RPL11*.

(E) The RNA stability assay in (D) was repeated with the A375-HEXIM1 cell line treated with DMSO or 1 μg/ml doxycycline to induce HEXIM1 expression for 24 hr (mean of three replicates ± SD). See also Figure S7 and Table S3.

expression with the transcripts differentially bound by iCLIP. We found a positive correlation between transcripts that were upregulated by nucleotide stress in RNA-seq and transcripts bound more strongly by HEXIM1 under nucleotide stress (Figure S7B; Table S3). When comparing these transcripts to a list of GRO-seq genes that had increased transcriptional activity (TR fold change < 0.7) upon nucleotide stress, 116 genes, such as *CDKN1A*, were transcriptionally activated and increasingly bound by HEXIM1 (Figure S7C). Knockdown of *HEXIM1* and *HEXIM2* partially rescued the increased expression of these transcripts that were increasingly bound by HEXIM1 under nucleotide stress, such as *CDKN1A* and *PTEN* (Figure 7C). We detected genes such as *CCNT2* that were bound by HEXIM1 and did not show any significant binding change under nucleotide stress (Figure 7B). These genes were not upregulated in RNA-seq and knockdown of *HEXIM1* and *HEXIM2* did not alter their expression (Figure 7C). This suggests that HEXIM1 differen-

ential binding stabilizes upregulated mRNAs to maintain their levels.

Anti-tumorigenic Transcripts Are Stabilized by HEXIM1 Binding

To investigate if the HEXIM1 binding shift to mRNA species upregulated by nucleotide stress stabilizes these RNAs, we performed an RNA stability assay where actinomycin D is added to halt the production of new transcripts so that degradation of steady-state transcripts can be observed. We performed this experiment with A771726 treatment and *HEXIM1/HEXIM2* knockdown. We observed that transcripts of *CDKN1A* and *PTEN* underwent a faster rate of degradation with *HEXIM1/HEXIM2* knocked down (Figure 7D). Conversely, the rate of degradation of *CCNT2* mRNA was unchanged (Figure 7D). We performed a complementary RNA stability experiment in the context of *HEXIM1* overexpression in the A375-HEXIM1 cell line. With *HEXIM1* overexpression, *CDKN1A* and *PTEN* transcripts underwent a slower rate of degradation, while *CCNT2* remained unchanged (Figure 7E).

Gene ontology analysis of HEXIM1-bound transcripts that were enriched in either the DMSO or A771726 condition revealed that apoptotic transcripts were enriched in nucleotide stress conditions, while homeostatic cell maintenance pathways were enriched at steady state (Figure S7D). We propose that

differential binding of HEXIM1 to certain transcripts like *CDKN1A* and *PTEN* stabilizes them under nucleotide stress. Other transcripts like *CCNT2* that do not experience differential binding are not affected.

DISCUSSION

HEXIM1 Is a Tumor Suppressor in Melanoma

Our work establishes a physiological role for HEXIM1 in melanoma in vivo, although further genetic validation in a mammalian system is needed. HEXIM1 was discovered as an upregulated gene upon treatment of cells with HMBA (Kusuhara et al., 1999). HMBA induces differentiation in a variety of cancer cell lines and primary human cancer cell cultures (Marks and Rifkind, 1989). HEXIM1 upregulation is correlated with the transition of cancer cells from proliferation to differentiation, and it has been studied in breast cancer (Ketchart et al., 2013; Wittmann et al., 2003, 2005; Yeh et al., 2013) and prostate cancer (Mascareno et al., 2012). 7SK snRNP member *LARP7* is mutated in gastric cancer (He et al., 2008; Mori et al., 2002). Rapidly dividing cancer cells are addicted to P-TEFb for proliferative gene expression, where loss of P-TEFb activity leads to growth arrest and apoptosis (Kryštof et al., 2012). This explains the efficacy of anti-cancer agents HMBA, suberoylanilide hydroxamic acid, and JQ1 that modulate HEXIM1 sequestration of P-TEFb (Bartholomeeusen et al., 2012). HEXIM1 is an important tumor suppressor that dampens excessive P-TEFb activity in cancer.

The ability for HEXIM1 to respond to cellular stress and participate in a transcriptional transition has great significance in tumorigenesis. Using DHODH inhibitors to create cellular stress by nucleotide starvation upregulates HEXIM1, reducing transcription elongation at genes associated with survival and proliferation. In addition, apoptotic genes upregulated by cellular stress can be stabilized by HEXIM1 binding, reinforcing the shift to a growth-suppressive transcriptional state. Metabolic drugs such as lef that induce HEXIM1 can transcriptionally inhibit numerous expressed genes simultaneously, targeting multiple pathways to halt cancer progression. Inducing the *HEXIM1* stress pathway can modulate gene expression through transcription elongation to treat cancer.

Each cell type has an Achilles' heel for stress, and the neural crest is sensitive to low nucleotides, as illustrated by patients with Miller's syndrome with DHODH mutations and consequent neural crest defects (Ng et al., 2010). Other cell types may be susceptible to different cellular stresses and respond in a similar manner by activating HEXIM1, reducing productive elongation to help the cell repair or undergo programmed cell death. Finding such dependencies in other cancers could lead to the development of new cancer therapies.

HEXIM1 Couples Nucleotide Metabolism with Transcriptional Regulation

When cells are nucleotide starved, transcription is slowed to conserve nucleotides until homeostasis returns. We suggest that one mechanism in which cells conserve nucleotides is to repress transcription elongation, which involves upregulating HEXIM1 to sequester P-TEFb. Increased binding of stress

response transcription factor SP1 to the *HEXIM1* promoter upregulates *HEXIM1* in response to nucleotide stress. Newly synthesized HEXIM1 sequesters P-TEFb away from gene promoters, leading to fewer phosphorylated Pol II molecules entering productive elongation. *HEXIM1* expression is tightly linked to nucleotide levels, with decreased nucleotides triggering an increase in *HEXIM1* expression. Cells can take advantage of the transcriptional reprieve, provided by HEXIM1-induced elongation inhibition, until nucleotides return to sufficient levels. HEXIM1 then returns to homeostatic levels, allowing transcription to return to normal. This suggests a feedback mechanism where cells control transcription based on the amount of mRNA precursors available. Cells slow their growth rate via HEXIM1 downregulation of genes associated with proliferation in times of starvation, conserving cellular resources until conditions become favorable.

There are advantages to regulating transcription elongation as a direct consequence of nucleotide starvation or other cellular stresses. Genes in the *Drosophila* embryo involved in key developmental pathways as well as heat shock genes are held in a paused state before induction (Adelman and Lis, 2012). At these genes, transcription has already been initiated as Pol II is recruited to the promoters. Pol II does not immediately transition to a productive elongation phase and, instead, remains paused on these promoters before receiving signals to induce productive elongation (Chopra et al., 2009; Muse et al., 2007; Zeitlinger et al., 2007). This poises Pol II at genes that require rapid induction (Adelman and Lis, 2012).

Such a system is highly beneficial to the organism as a quick and concerted response could limit the damage done by the stress. With nucleotide starvation, unfavorable effects might include DNA damage, mis-expression of mRNA and protein, and possibly bioenergetic issues due to the lack of ATP and GTP. An immediate repression of non-essential genes by halting elongation through HEXIM1 sequestration of P-TEFb allows for stress response genes to be preferentially expressed with the remaining nucleotides available. Inhibiting transcription elongation with nucleotide starvation is a viable mechanism to ensure a quick response to avoid damage from cellular stress. HEXIM1 has been shown to respond to environmental stimuli such as UV light, signaling cascades, and transcriptional perturbations by various inhibitors (Peterlin et al., 2012). Our study, together with others, proposes that HEXIM1 is a general stress sensor that responds to cellular stress by modulating gene expression to achieve an appropriate response.

HEXIM1 Facilitates Switching of Gene Expression Programs

Our study establishes a second function of HEXIM1 of binding mRNAs to promote a gene expression transition. If nucleotide starvation continues at an unsustainable rate, programmed cell death occurs. Apoptotic genes become upregulated as a result and HEXIM1 can bind and stabilize these transcripts, reinforcing apoptotic gene expression. Other than binding 7SK to nucleate the 7SK snRNP and sequester P-TEFb, HEXIM1 can act as a modulator of specific RNA species under different gene expression programs.

The dual functionality of HEXIM1 might explain its importance in differentiation, where HEXIM1 is significantly upregulated

(Marks and Rifkind, 1989). During differentiation, proliferation genes are downregulated and genes responsible for downstream cell fate are upregulated. This second function of HEXIM1 also could explain why rapidly dividing cancer cells undergo growth arrest and apoptosis under P-TEFb inhibition by drugs. HEXIM1 induction inhibits P-TEFb, similar to treatment with CDK9 inhibitors, to inhibit cancer-associated gene expression. In addition, it stabilizes apoptotic transcripts to promote growth arrest and cell death. The fact that not all HEXIM1-bound transcripts are stabilized by HEXIM1 suggests the presence of additional factors that are recruited to specific transcripts by unknown mechanisms to aid in HEXIM1-mediated RNA stabilization. HEXIM1 plays an important role in differentiation and tumor suppression by reducing productive elongation of proliferation genes and promoting the expression of cell fate or apoptotic genes, respectively, thereby facilitating a transition from one gene expression program to the next.

EXPERIMENTAL PROCEDURES

Animal maintenance and experiments were performed in accordance with the Institutional Animal Care and Use Committee (IACUC) guidelines and with IACUC approval at Boston Children's Hospital (zebrafish) and Beth Israel Deaconess Medical Center (mouse).

MiniCoopR Assay

The MiniCoopR vector sequence and construction was described previously (Ceol et al., 2011). MiniCoopR vectors and Tol2 transposase mRNA were microinjected into one-cell zebrafish embryos generated from an incross of *Tg(mitfa:BRAF^{V600E});p53^{-/-};mitfa^{-/-}* zebrafish. Rescued animals were scored weekly for the presence of visible tumors. For *hexim* deletion, the MiniCoopR vector was engineered to express Cas9 under the control of a *mitfa* promoter in order to achieve melanocyte-specific gene targeting. A gRNA efficiently mutating *hexim* was expressed off a *U6* promoter while a gRNA against *p53* was used as a negative control (Ablain et al., 2015). The two vectors were injected into one-cell-stage *Tg(mitfa:BRAF^{V600E});p53^{-/-};mitfa^{-/-}* embryos, and tumor formation was monitored.

GRO-Seq Sample Preparation and Sequencing

GRO-seq was performed as previously described (Kim et al., 2013) with conditions optimized for A375 cells. One million A375 cells were treated with DMSO, 25 μ M lef, or 25 μ M A771726. After 48-hr treatment, cells were washed, swelled, and lysed in lysis buffer with IGEPAL detergent. Cells were frozen down, nuclear run-on reaction was performed, and nascent RNA was isolated and sequenced.

ChIP-Seq Sample Preparation and Sequencing

ChIP-seq and ChIP-reChIP were performed as previously described (Batsché et al., 2006; Lee et al., 2006) with conditions optimized for A375 cells. One hundred million A375 cells per condition were treated with DMSO or 25 μ M A771726. After 48-hr treatment, cells were fixed in formaldehyde and subjected to ChIP with HEXIM1, CDK9, POLR2A, or SP1 antibodies. For reChIP experiments, eluates were diluted to reduce the SDS concentration before the subsequent immunoprecipitation was performed. Input DNA (10 μ l) and the entire volume of ChIP DNA samples were prepared for sequencing.

FAST-iCLIP

FAST-iCLIP was performed as described previously (Flynn et al., 2015) with some modifications. A375 cells were cultured and treated with DMSO or 25 μ M A771726 for 48 hr, then ultraviolet C crosslinked. Each iCLIP experiment was normalized for total protein amount and partially digested with RNaseI. To isolate HEXIM1-bound RNAs, HEXIM1 antibody conjugated to Protein A Dynabeads was incubated with RNaseI-digested lysates overnight at 4°C on rotation. Immunoprecipitation, washing, and

subsequent biochemical and library preparation steps were carried out for sequencing.

ACCESSION NUMBERS

The accession number for the GRO-seq, ChIP-seq, RNA-seq, and FAST-iCLIP sequencing data reported in this paper is GEO: GSE68053.

SUPPLEMENTAL INFORMATION

Supplemental Information includes Supplemental Experimental Procedures, seven figures, and four tables and can be found with this article online at <http://dx.doi.org/10.1016/j.molcel.2016.03.013>.

AUTHOR CONTRIBUTIONS

Conceptualization, J.L.T. and L.I.Z.; Supervision, J.L.T., R.M.W., D.H.P., P.P.P., B.M.P., T.H.K., J.M.A., H.Y.C., R.A.Y., and L.I.Z.; Funding Acquisition & Resources, L.I.Z., D.H.P., P.P.P., B.M.P., Y.Z., T.H.K., J.M.A., H.Y.C., and R.A.Y.; Writing – Original Draft, J.L.T.; Writing – Review & Editing, J.L.T. and L.I.Z.; Methodology, J.L.T. and L.I.Z.; Investigation, J.L.T., R.D.F., R.A.F., J.A., S.Y., V.S.-A., Z.P.F., B.T.D., A.C.L., K.F., C.S., C.B.G., Y.J.K., J.G.C., A.B., N.P., S.A., J.E.B., E.v.R., E.J.H., and N.S.-C.; Formal Analysis, J.L.T., R.A.Y., S.Y., and C.B.G.

ACKNOWLEDGMENTS

We thank Min Yuan for her help with the metabolomics studies and Dr. Telmo Henriques for his advice on RNA assays. This work was supported by the Howard Hughes Medical Institute and the National Cancer Institute (NIH) R01CA103846 (to L.I.Z.). L.I.Z. is a founder and stockholder of Fate, Inc.; Scholar Rock; and a scientific advisor for Stemgent. J.L.T. is an Agency for Science, Technology & Research, Singapore National Science Scholarship recipient. C.B.G. is a PhRMA Foundation predoctoral fellow. R.A.Y. is a founder and stockholder of Syros Pharmaceuticals. This work was partially supported by NIH grants 2P01CA120964 (to J.M.A.), 5P30CA006516 (to J.M.A.), R01CA140485 (to T.H.K.), R21AI107067 (to T.H.K.), R01-ES023168 (to H.Y.C.), and R01-HG004361 (to H.Y.C.).

Received: November 4, 2015

Revised: February 2, 2016

Accepted: March 10, 2016

Published: April 7, 2016

REFERENCES

- Ablain, J., Durand, E.M., Yang, S., Zhou, Y., and Zon, L.I. (2015). A CRISPR/Cas9 vector system for tissue-specific gene disruption in zebrafish. *Dev. Cell* 32, 756–764.
- Adelman, K., and Lis, J.T. (2012). Promoter-proximal pausing of RNA polymerase II: emerging roles in metazoans. *Nat. Rev. Genet.* 13, 720–731.
- Alazami, A.M., Al-Owain, M., Alzahrani, F., Shuaib, T., Al-Shamrani, H., Al-Falki, Y.H., Al-Qahtani, S.M., Alsheddi, T., Colak, D., and Alkuraya, F.S. (2012). Loss of function mutation in LARP7, chaperone of 7SK ncRNA, causes a syndrome of facial dysmorphism, intellectual disability, and primordial dwarfism. *Hum. Mutat.* 33, 1429–1434.
- Barboric, M., Lenasi, T., Chen, H., Johansen, E.B., Guo, S., and Peterlin, B.M. (2009). 7SK snRNP/P-TEFb couples transcription elongation with alternative splicing and is essential for vertebrate development. *Proc. Natl. Acad. Sci. USA* 106, 7798–7803.
- Bartholomeussen, K., Xiang, Y., Fujinaga, K., and Peterlin, B.M. (2012). Bromodomain and extra-terminal (BET) bromodomain inhibition activate transcription via transient release of positive transcription elongation factor b (P-TEFb) from 7SK small nuclear ribonucleoprotein. *J. Biol. Chem.* 287, 36609–36616.

- Batsché, E., Yaniv, M., and Muchardt, C. (2006). The human SWI/SNF subunit Brm is a regulator of alternative splicing. *Nat. Struct. Mol. Biol.* *13*, 22–29.
- Ceol, C.J., Houvras, Y., Jane-Vaibuena, J., Bilodeau, S., Orlando, D.A., Battisti, V., Fritsch, L., Lin, W.M., Hollmann, T.J., Ferré, F., et al. (2011). The histone methyltransferase SETDB1 is recurrently amplified in melanoma and accelerates its onset. *Nature* *471*, 513–517.
- Chabosseau, P., Buhagiar-Labarchède, G., Onclercq-Delic, R., Lambert, S., Debatisse, M., Brison, O., and Amor-Guélet, M. (2011). Pyrimidine pool imbalance induced by BLM helicase deficiency contributes to genetic instability in Bloom syndrome. *Nat. Commun.* *2*, 368.
- Chang, L., Guo, R., Huang, Q., and Yen, Y. (2013). Chromosomal instability triggered by Rrm2b loss leads to IL-6 secretion and plasmacytic neoplasms. *Cell Rep.* *3*, 1389–1397.
- Chopra, V.S., Hong, J.-W., and Levine, M. (2009). Regulation of Hox gene activity by transcriptional elongation in *Drosophila*. *Curr. Biol.* *19*, 688–693.
- Contreras, X., Barboric, M., Lenasi, T., and Peterlin, B.M. (2007). HMBA releases P-TEFb from HEXIM1 and 7SK snRNA via PI3K/Akt and activates HIV transcription. *PLoS Pathog.* *3*, 1459–1469.
- Creusot, F., Acs, G., and Christman, J.K. (1982). Inhibition of DNA methyltransferase and induction of Friend erythroleukemia cell differentiation by 5-azacytidine and 5-aza-2'-deoxycytidine. *J. Biol. Chem.* *257*, 2041–2048.
- ENCODE Project Consortium (2012). An integrated encyclopedia of DNA elements in the human genome. *Nature* *489*, 57–74.
- Flynn, R.A., Martin, L., Spitalo, R.C., Do, B.T., Sagan, S.M., Zarnegar, B., Qu, K., Khavari, P.A., Quake, S.R., Sarnow, P., and Chang, H.Y. (2015). Dissecting noncoding and pathogen RNA-protein interactomes. *RNA* *21*, 135–143.
- Fujinaga, K., Irwin, D., Huang, Y., Taube, R., Kurosu, T., and Peterlin, B.M. (2004). Dynamics of human immunodeficiency virus transcription: P-TEFb phosphorylates RD and dissociates negative effectors from the transactivation response element. *Mol. Cell Biol.* *24*, 787–795.
- Guo, J., and Price, D.H. (2013). RNA polymerase II transcription elongation control. *Chem. Rev.* *113*, 8583–8603.
- He, N., Jahchan, N.S., Hong, E., Li, Q., Bayfield, M.A., Maraia, R.J., Luo, K., and Zhou, Q. (2008). A La-related protein modulates 7SK snRNP integrity to suppress P-TEFb-dependent transcriptional elongation and tumorigenesis. *Mol. Cell* *29*, 588–599.
- Huang, W.-Y., Hsu, S.-D., Huang, H.-Y., Sun, Y.-M., Chou, C.-H., Weng, S.-L., and Huang, H.-D. (2015). MethHC: a database of DNA methylation and gene expression in human cancer. *Nucleic Acids Res.* *43*, D856–D861.
- Jeronimo, C., Forget, D., Bouchard, A., Li, Q., Chua, G., Poitras, C., Thérien, C., Bergeron, D., Bourassa, S., Greenblatt, J., et al. (2007). Systematic analysis of the protein interaction network for the human transcription machinery reveals the identity of the 7SK capping enzyme. *Mol. Cell* *27*, 262–274.
- Kawakami, Y., Eliyahu, S., Delgado, C.H., Robbins, P.F., Sakaguchi, K., Appella, E., Yannelli, J.R., Adema, G.J., Miki, T., and Rosenberg, S.A. (1994). Identification of a human melanoma antigen recognized by tumor-infiltrating lymphocytes associated with *in vivo* tumor rejection. *Proc. Natl. Acad. Sci. USA* *91*, 6458–6462.
- Ketchart, W., Smith, K.M., Krupka, T., Wittmann, B.M., Hu, Y., Rayman, P.A., Doughman, Y.Q., Albert, J.M., Bai, X., Finke, J.H., et al. (2013). Inhibition of metastasis by HEXIM1 through effects on cell invasion and angiogenesis. *Oncogene* *32*, 3829–3839.
- Kim, Y.J., Greer, C.B., Cecchini, K.R., Harris, L.N., Tuck, D.P., and Kim, T.H. (2013). HDAC inhibitors induce transcriptional repression of high copy number genes in breast cancer through elongation blockade. *Oncogene* *32*, 2828–2835.
- Kryštof, V., Baumli, S., and Fürst, R. (2012). Perspective of cyclin-dependent kinase 9 (CDK9) as a drug target. *Curr. Pharm. Des.* *18*, 2883–2890.
- Kusuhara, M., Nagasaki, K., Kimura, K., Maass, N., Manabe, T., Ishikawa, S., Aikawa, M., Miyazaki, K., and Yamaguchi, K. (1999). Cloning of hexamethylene-bis-acetamide-inducible transcript, HEXIM1, in human vascular smooth muscle cells. *Biomed. Res.* *20*, 273–279.
- Lee, T.I., Johnstone, S.E., and Young, R.A. (2006). Chromatin immunoprecipitation and microarray-based analysis of protein location. *Nat. Protoc.* *1*, 729–748.
- Lin, W.M., Baker, A.C., Beroukhim, R., Winckler, W., Feng, W., Marmion, J.M., Laine, E., Greulich, H., Tseng, H., Gates, C., et al. (2008). Modeling genomic diversity and tumor dependency in malignant melanoma. *Cancer Res.* *68*, 664–673.
- Liu, W., Le, A., Hancock, C., Lane, A.N., Dang, C.V., Fan, T.W.-M., and Phang, J.M. (2012). Reprogramming of proline and glutamine metabolism contributes to the proliferative and metabolic responses regulated by oncogenic transcription factor c-MYC. *Proc. Natl. Acad. Sci. USA* *109*, 8983–8988.
- Liu, P., Xiang, Y., Fujinaga, K., Bartholomeeusen, K., Nilson, K.A., Price, D.H., and Peterlin, B.M. (2014). Release of positive transcription elongation factor b (P-TEFb) from 7SK small nuclear ribonucleoprotein (snRNP) activates hexamethylene bisacetamide-inducible protein (HEXIM1) transcription. *J. Biol. Chem.* *289*, 9918–9925.
- Marks, P.A., and Rifkin, R.A. (1989). Induced differentiation of erythroleukemia cells by hexamethylene bisacetamide: a model for cytodifferentiation of transformed cells. *Environ. Health Perspect.* *80*, 181–188.
- Marshall, N.F., Peng, J., Xie, Z., and Price, D.H. (1996). Control of RNA polymerase II elongation potential by a novel carboxyl-terminal domain kinase. *J. Biol. Chem.* *271*, 27176–27183.
- Mascareno, E.J., Belashov, I., Siddiqui, M.A.Q., Liu, F., and Dhar-Mascareno, M. (2012). Hexim-1 modulates androgen receptor and the TGF- β signaling during the progression of prostate cancer. *Prostate* *72*, 1035–1044.
- McClelland, R.A., Finlay, P., Walker, K.J., Nicholson, D., Robertson, J.F., Blamey, R.W., and Nicholson, R.I. (1990). Automated quantitation of immunocytochemically localized estrogen receptors in human breast cancer. *Cancer Res.* *50*, 3545–3550.
- Meuth, M. (1989). The molecular basis of mutations induced by deoxyribonucleoside triphosphate pool imbalances in mammalian cells. *Exp. Cell Res.* *181*, 305–316.
- Mori, Y., Sato, F., Selaru, F.M., Oлару, A., Perry, K., Kimos, M.C., Tamura, G., Matsubara, N., Wang, S., Xu, Y., et al. (2002). Instability typing reveals unique mutational spectra in microsatellite-unstable gastric cancers. *Cancer Res.* *62*, 3641–3645.
- Muse, G.W., Gilchrist, D.A., Nechaev, S., Shah, R., Parker, J.S., Grissom, S.F., Zeitlinger, J., and Adelman, K. (2007). RNA polymerase is poised for activation across the genome. *Nat. Genet.* *39*, 1507–1511.
- Ng, S.B., Buckingham, K.J., Lee, C., Bigham, A.W., Tabor, H.K., Dent, K.M., Huff, C.D., Shannon, P.T., Jabs, E.W., Nickerson, D.A., et al. (2010). Exome sequencing identifies the cause of a mendelian disorder. *Nat. Genet.* *42*, 30–35.
- Peterlin, B.M., Brogie, J.E., and Price, D.H. (2012). 7SK snRNA: a noncoding RNA that plays a major role in regulating eukaryotic transcription. *Wiley Interdiscip. Rev. RNA* *3*, 92–103.
- Rahl, P.B., Lin, C.Y., Seila, A.C., Flynn, R.A., McQuine, S., Burge, C.B., Sharp, P.A., and Young, R.A. (2010). c-Myc regulates transcriptional pause release. *Cell* *141*, 432–445.
- Raskin, L., Fullen, D.R., Giordano, T.J., Thomas, D.G., Frohm, M.L., Cha, K.B., Ahn, J., Mukherjee, B., Johnson, T.M., and Gruber, S.B. (2013). Transcriptome profiling identifies HMGA2 as a biomarker of melanoma progression and prognosis. *J. Invest. Dermatol.* *133*, 2585–2592.
- Rhodes, D.R., Yu, J., Shanker, K., Deshpande, N., Varambally, R., Ghosh, D., Barrette, T., Pandey, A., and Chinnaiyan, A.M. (2004). ONCOMINE: a cancer microarray database and integrated data-mining platform. *Neoplasia* *6*, 1–6.
- Ryu, H., Lee, J., Zaman, K., Kubiliis, J., Ferrante, R.J., Ross, B.D., Neve, R., and Ratan, R.R. (2003). Sp1 and Sp3 are oxidative stress-inducible, antideath transcription factors in cortical neurons. *J. Neurosci.* *23*, 3597–3606.

- Talantov, D., Mazumder, A., Yu, J.X., Briggs, T., Jiang, Y., Backus, J., Atkins, D., and Wang, Y. (2005). Novel genes associated with malignant melanoma but not benign melanocytic lesions. *Clin. Cancer Res.* *11*, 7234–7242.
- Weinberg, G., Ullman, B., and Martin, D.W., Jr. (1981). Mutator phenotypes in mammalian cell mutants with distinct biochemical defects and abnormal deoxyribonucleoside triphosphate pools. *Proc. Natl. Acad. Sci. USA* *78*, 2447–2451.
- White, R.M., Cech, J., Ratanasirintraooot, S., Lin, C.Y., Rahl, P.B., Burke, C.J., Langdon, E., Tomlinson, M.L., Mosher, J., Kaufman, C., et al. (2011). DHODH modulates transcriptional elongation in the neural crest and melanoma. *Nature* *471*, 518–522.
- Wittmann, B.M., Wang, N., and Montano, M.M. (2003). Identification of a novel inhibitor of breast cell growth that is down-regulated by estrogens and decreased in breast tumors. *Cancer Res.* *63*, 5151–5158.
- Wittmann, B.M., Fujinaga, K., Deng, H., Ogba, N., and Montano, M.M. (2005). The breast cell growth inhibitor, estrogen down regulated gene 1, modulates a novel functional interaction between estrogen receptor alpha and transcriptional elongation factor cyclin T1. *Oncogene* *24*, 5576–5588.
- Yamada, T., Yamaguchi, Y., Inukai, N., Okamoto, S., Mura, T., and Handa, H. (2006). P-TEFb-mediated phosphorylation of hSpt5 C-terminal repeats is critical for processive transcription elongation. *Mol. Cell* *21*, 227–237.
- Yeh, I.-J., Ogba, N., Bensigner, H., Welford, S.M., and Montano, M.M. (2013). HEXIM1 down-regulates hypoxia-inducible factor-1 α protein stability. *Biochem. J.* *456*, 195–204.
- Yik, J.H.N., Chen, R., Nishimura, R., Jennings, J.L., Link, A.J., and Zhou, Q. (2003). Inhibition of P-TEFb (CDK9/Cyclin T) kinase and RNA polymerase II transcription by the coordinated actions of HEXIM1 and 7SK snRNA. *Mol. Cell* *12*, 971–982.
- Zeitlinger, J., Stark, A., Kellis, M., Hong, J.-W., Nechaev, S., Adelman, K., Levine, M., and Young, R.A. (2007). RNA polymerase stalling at developmental control genes in the *Drosophila melanogaster* embryo. *Nat. Genet.* *39*, 1512–1516.
- Zhang, W.C., Shyh-Chang, N., Yang, H., Rai, A., Umashankar, S., Ma, S., Soh, B.S., Sun, L.L., Tai, B.C., Nga, M.E., et al. (2012). Glycine decarboxylase activity drives non-small cell lung cancer tumor-initiating cells and tumorigenesis. *Cell* *148*, 259–272.